



Biomaterials for orthopedics: anti-biofilm activity of a new bioactive glass coating on titanium implants

Daniella Maia Marques, Viviane de Cássia Oliveira, Marina Trevelin Souza, Edgar Dutra Zanotto, João Paulo Mardegan Issa & Evandro Watanabe

To cite this article: Daniella Maia Marques, Viviane de Cássia Oliveira, Marina Trevelin Souza, Edgar Dutra Zanotto, João Paulo Mardegan Issa & Evandro Watanabe (2020) Biomaterials for orthopedics: anti-biofilm activity of a new bioactive glass coating on titanium implants, *Biofouling*, 36:2, 234-244, DOI: [10.1080/08927014.2020.1755842](https://doi.org/10.1080/08927014.2020.1755842)

To link to this article: <https://doi.org/10.1080/08927014.2020.1755842>



Published online: 22 Apr 2020.



Submit your article to this journal [↗](#)



Article views: 10



View related articles [↗](#)



View Crossmark data [↗](#)



Biomaterials for orthopedics: anti-biofilm activity of a new bioactive glass coating on titanium implants

Daniella Maia Marques^a , Viviane de Cássia Oliveira^{a,b} , Marina Trevelin Souza^c ,
Edgar Dutra Zanotto^c , João Paulo Mardegan Issa^d  and Evandro Watanabe^{a,e} 

^aDepartment of General and Specialized Nursing, College of Nursing of Ribeirão Preto, University of São Paulo, Ribeirão Preto, São Paulo, Brazil; ^bDepartment of Dental Materials and Prostheses, School of Dentistry of Ribeirão Preto, University of São Paulo, Ribeirão Preto, São Paulo, Brazil; ^cVitreous Materials Laboratory, Department of Materials Engineering, Federal University of São Carlos, São Carlos, São Paulo, Brazil; ^dDepartment of Morphology, Physiology and Basic Pathology, School of Dentistry of Ribeirão Preto, University of São Paulo, Ribeirão Preto, São Paulo, Brazil; ^eDepartment of Restorative Dentistry, Network in Exposome Human and Infectious Diseases, School of Dentistry of Ribeirão Preto, University of São Paulo, Ribeirão Preto, São Paulo, Brazil

ABSTRACT

This study evaluated adhesion and biofilm formation by *Candida albicans*, *Pseudomonas aeruginosa* and *Staphylococcus epidermidis* on surfaces of titanium (Ti) and titanium coated with F18 Bioactive Glass (BGF18). Biofilms were grown and the areas coated with biofilm were determined after 2, 4 and 8 h. Microscopy techniques were applied in order to visualize the structure of the mature biofilm and the extracellular matrix. On the BGF18 specimens, there was less biofilm formation by *C. albicans* and *S. epidermidis* after incubation for 8 h. For *P. aeruginosa* biofilm, a reduction was observed after incubation for 4 h, and it remained reduced after 8 h on BGF18 specimens. All biofilm matrices seemed to be thicker on BGF18 surface than on titanium surfaces. BGF18 showed significant anti-biofilm activity in comparison with Ti in the initial periods of biofilm formation; however, there was extensive biofilm after incubation for 48 h.

ARTICLE HISTORY

Received 7 October 2019
Accepted 8 April 2020

KEYWORDS

Biofilms; *Candida albicans*;
Pseudomonas aeruginosa;
Staphylococcus epidermidis;
Bioactive glass

Introduction

A common complication in the postoperative period of orthopedic surgeries is the infection associated with metallic implants, with obvious health and financial setbacks. Frequently, the infections can lead to implant removal and fatalities (Gao et al. 2014; Cochis et al. 2016). The most commonly used approach in the treatment of these infections is anti-biobiotic therapy. Nonetheless, after biofilm forms on the implant surface, antibiotics may lose their efficacy and thereby reduce antibacterial activity (Kuehl et al. 2016).

The organization of microorganisms in biofilms emerges as a strategy to survival in different environments and on different surfaces. The potential for persistence and survival of biofilms is due to the mechanical cohesive stability provided by filling the space between the bacteria with extracellular polymeric substances known as the extracellular matrix (Kragh et al. 2016). According to Macia et al. (2014), when cells are organized in biofilms, their tolerance to antimicrobial agents is about 100–1,000 times

greater compared with the planktonic form. In addition, there is a greater proportion of bacteria living in biofilms than in the planktonic form. Currently, it is believed that the standard bacterial lifestyle is in biofilm, and the planktonic cells would be only a transitional phase in the microorganism life cycle (Kragh et al. 2016). In this way, the use of surfaces capable of preventing or reducing bacterial colonization is considered a necessary and unavoidable requirement in the health field.

Since the first report of bioactive glass in 1969 (Bioglass®45S5) (Hench et al. 1971) different compositions have been proposed for various applications (Drago et al. 2018). The current scenario shows several clinical products, which have been used, mainly in orthopedics and dentistry (Baino et al. 2018). Additionally, soft tissue engineering applications, such as wound dressings, regeneration of cardiac, pulmonary and gastrointestinal tissues have been reported (Miguez-Pacheco et al. 2015; Kargozar et al. 2017). However, there is a plethora of new applications of bioactive glasses yet to be studied to find new answers to the challenges of biofilms associated with implants.

F18 Bioactive Glass (BGF18) is a newly developed glass composition that belongs to the system $\text{SiO}_2\text{-Na}_2\text{O-K}_2\text{O-CaO-MgO-P}_2\text{O}_5$ and has the physical-chemical characteristics necessary for the formation of fibers, powders, scaffolds, monoliths, among other possible formats. BGF18 has a wider range of workability than any other bioactive glasses, maintaining increased bioactivity and bactericidal properties (Souza et al. 2016a, 2017). By using this glass, it was possible to design various types of devices, such as membranes for wound healing, nerve conduction guidance, highly porous scaffolds and coating metallic implants (Souza et al. 2017; Souza et al. 2016b; Gabbai-Armelin et al. 2017; Soares et al. 2018). These devices were evaluated for their ability to stimulate tissue proliferation and regeneration with improved biointeraction and easy handling during implantation (Souza et al. 2017; Gabbai-Armelin et al. 2017).

The mechanical strength, bioactivity, wettability, degradation, and permeability of BGF18 were characterized by Souza et al. (2016b). In addition, Gabbai-Armelin et al. (2017) conducted a characterization of the BGF18 scaffold in terms of porosity, mineralization and morphological features. The authors suggested a substantial reduction in the contact angle and an improvement of wetting behavior. These effects can lead to a superior biointeraction with the biological environment *in vivo*, facilitating the tissue regeneration process.

Coating metallic implants is an interesting process for clinical applications, since BGF18 coating has been shown to induce positive results regarding osseointegration. Soares et al. (2018) showed that BGF18 titanium-coated implants had improved wettability and enhanced both bone-implant contact and bone density after only 2 weeks post-implantation. However, up to the present date, no tests have been conducted regarding the anti-biofilm potential of BGF18 when used as a coating material. Thus, the objective of this study was to evaluate *in vitro* the adhesion and formation of biofilm by *Candida albicans*, *Pseudomonas aeruginosa* and *Staphylococcus epidermidis* on specimens of titanium and titanium coated with BGF18. The null hypothesis of this study is that the coating with BGF18 does not alter cellular adhesion and formation of biofilm on the titanium surface.

Materials and methods

Sample preparation

The F18 Bioactive Glass (BGF18) composition belongs to the system $\text{SiO}_2\text{-Na}_2\text{O-K}_2\text{O-MgO-CaO-P}_2\text{O}_5$, and its manufacturing processes were described by Souza et al. (2017). Briefly, bioglass was produced by

melting and casting, the cm-sized pieces were then milled, and the resulting powder was sieved. The mean diameter of the powder particles was $\cong 50 \mu\text{m}$. For coating, first, both the sample surfaces of 132 circular titanium samples ($10 \times 4 \text{ mm}$) were standardized using 400# sandpaper. Then, a layer of the biomaterial powder was applied to the surface of 66 samples. The deposition of this layer was done using the pneumatic atomization technique. Sixty-six non-coated circular titanium samples were used as controls.

Surface roughness measurements were performed for both coated and non-coated samples ($n=10$), by using a surface roughness tester (Mitutoyo, Tokyo, Japan). By moving a diamond tip (speed: 0.5 mm s^{-1} ; distance: 4.8 mm; length reading: 4.0 mm), three readings were performed with an incremental distance of 1 mm between each reading line. Roughness value was defined as the mean of the three values (Ra) obtained.

For sterilization, the specimens were distributed in glass Petri dishes ($90 \times 15 \text{ mm}$) and placed in a Pasteur's oven at 160°C for 2 h. This sample features were chosen because of the results obtained in previous studies by Soares et al. (2018). Three samples of each type of material (titanium and titanium coated with BGF18) were submitted to the sterility test. Each sample was immersed in 200 ml of Tryptic Soy Broth – TSB (BD Difco, Sparks, MD, USA) and incubated at 37°C for 14 days. The samples were homogenized daily and the presence of turbidity in the culture medium was evaluated.

Culture conditions

Antimicrobial evaluation was carried out, in triplicate, against three strains from the American Type Culture Collection (ATCC): *Candida albicans* (10231), *Pseudomonas aeruginosa* (27853) and *Staphylococcus epidermidis* (12228). The culture media used for the growth of these microorganisms were Sabouraud Dextrose Broth/Agar (BD Difco), Tryptic Soy Broth/Agar (BD Difco) and Brain Heart Infusion Broth/Agar (BD Difco), respectively. The strains were thawed and plated onto Petri dishes ($60 \times 15 \text{ mm}$) containing the specific medium. The samples were incubated at 37°C for 48 h under aerobic conditions. One colony was transferred to broth medium and re-incubated at 37°C for 19–24 h in order to achieve exponential growth phase. Then, the cultures were centrifuged (4,200 g for 5 min) and washed twice in phosphate buffered saline (PBS).

The bacterial inoculum was prepared by reading the optical density in a Multiskan GO spectrophotometer (Thermo Scientific, MA, USA), at a wavelength of 625 nm. For the yeast, due to the variable morphology of the genus, counting was performed in a Neubauer chamber (HBG, Gießen, Germany) using an optical microscope (Carl Zeiss® Microscopy Ltd, Oberkochen, Germany). In a class II type A1 biological safety cabinet (VECO, Campinas, SP, Brazil), the specimens were randomly assigned in 24-well tissue culture plates (TPP, Trasadingen, Switzerland), and 1.5 ml of medium broth containing standardized cell suspension (10^6 CFU ml⁻¹) were added to each well. Hence, the bioglass mass/medium ratio used in this study was ~ 1.34 mg ml⁻¹. The plates were incubated at 37 °C in a shaker incubator (CienLab, Campinas, SP, Brazil) at 75 rpm.

Adhesion assay

For visualization of cell adhesion and biofilm formation, three specimens were analyzed after incubation for 2, 4 and 8 h using a fluorescence microscope (FM) (Carl Zeiss, Axio Observer A1). The samples were washed in PBS and stained for 15 min, protected from light, with the LIVE/DEAD™ Biofilm Viability Kit (Molecular Probes, Inc., Eugene, OR, USA) according to the manufacturer's protocol. Afterwards, the samples were washed twice with distilled water, and individual coverslips were positioned on the surface of the specimens for analysis under an inverted fluorescence microscope with the appropriate filters and a magnification of 630×. ZEN 2.3 lite software (Carl Zeiss) was used to capture the images. For each specimen, 20 images were taken at random sites. All images were analyzed by ImageJ software (National Institutes of Health, Madison, WI, USA) in order to measure the biofilm area (%).

Biofilm morphology

To evaluate biofilm morphology, confocal laser scanning microscopy (CLSM) and scanning electron microscopy (SEM) were performed. Samples after biofilm growth for 24 and 48 h were analyzed. For CLSM, the samples were stained with the LIVE/DEAD™ Biofilm Viability Kit according to the manufacturer's protocol. Confocal images were acquired randomly using a Leica TCS SP8 inverted microscope (Leica Microsystems, Wetzlar, Germany) at a magnification of 630×. Fluorochromes were excited at 488 and 540 nm, and images were acquired in the range

of 550–570 nm and 610–630 nm, respectively. To obtain SEM images, the samples were fixed with 2.5% glutaraldehyde for 60 min and then dehydrated in a graded ethanol series (30%, 50%, 70%, 90% and 100%, 10 min each). The surface morphology of the biofilms was examined at magnification of 500, 1,000 and 5,000× under high vacuum with a JEOL JSM-35CF microscope (Tokyo, Japan). Samples without biofilm formation were evaluated as control.

Biofilm matrix measurement

For matrix measurements, three specimens (after biofilm growth for 48 h) were processed for CLSM. The samples were stained with 1,000 µl of FilmTracer™ SYPRO Ruby Biofilm Matrix (Invitrogen). The samples were incubated in the dark for 30 min at room temperature and washed twice in distilled water. As a negative control for biofilm matrix formation, samples without biofilm were used. SYPRO Ruby was excited at the wavelength of 450 nm, and images were acquired in the range of 610–630 nm. A Z-series scan was acquired in 20 random fields, at a magnification of 630×. The Z-axis measurement was used to determine the maximum biofilm thickness. Therefore, the distance between the surface of the specimen and the last biofilm-related signal at bulk-biofilm-interface were measured during image acquisition (West et al. 2014). It is known that biofilms do not exhibit heterogeneous thickness throughout the surface and, thus, 20 random fields were measured for each condition. The values, in micrometers (µm), were computed for each condition. Z-stacks of confocal images were rendered into 3-D mode using the Leica LAS software.

Statistical analysis

Cell adhesion and the surface roughness data set did not exhibit normal distribution as inferred by the Shapiro–Wilk test. Cell adhesion was analyzed by multiple comparisons considering time (2, 4 and 8 h) and material (titanium and BGF18), in a Generalized Linear Model with Bonferroni correction. Surface roughness assay values were compared by the Mann–Whitney *U* test. Values referring to matrix thickness adhere to normal distribution and were compared by test *t*-Student. The statistical tests were performed through IBM SPSS Statistics 25.0 software (IBM Corp Armonk, NY, USA). The significance level was set at 0.05.

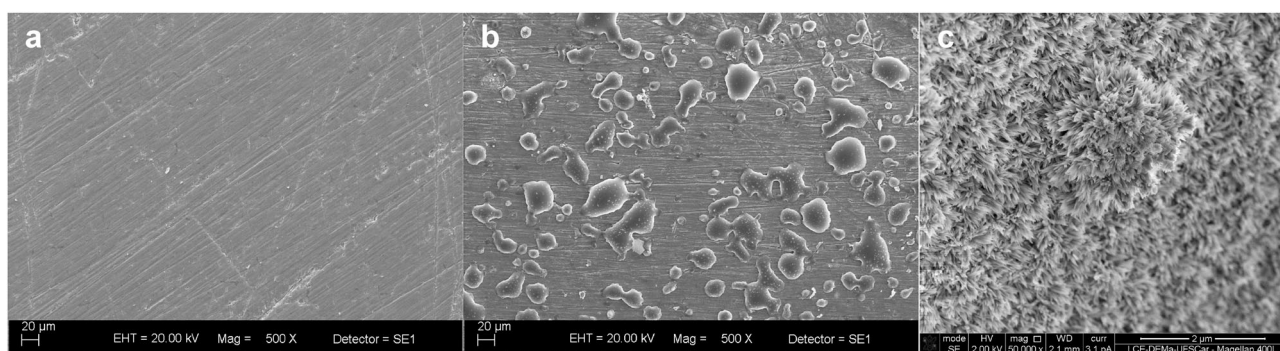


Figure 1. SEM images of Ti (a), BGF18 coating (b) and BGF18 after immersion for 16 h in Simulated Body Fluid, representing an initial dissolution of the biomaterial (c). Scale bars = 20 μm (a, b); 2 μm (c).

Table 1. Median values and 95% confidence intervals for means, as percentages, of the image areas coated with *C. albicans* (Ca), *P. aeruginosa* (Pa) and *S. epidermidis* (Se) after incubation for 2, 4 and 8 h on surfaces of titanium (Ti) and titanium coated with F18 Bioactive Glass (BGF18).

		2 h		4 h		8 h	
Ca	Ti	4.54 (4.41; 6.27)	$p = 1.000^*$	9.90 (10.52; 13.92)	$p = 1.000^*$	32.89 (29.38; 38.16)	$p < 0.001^*$
	BGF18	5.60 (4.97; 6.57)		14.40 (13.37; 16.51)		17.25 (16.79; 19.91)	
Pa	Ti	1.60 (1.41; 1.77)	$p = 0.794^*$	7.33 (7.28; 9.58)	$p < 0.001^*$	8.57 (8.68; 12.26)	$p < 0.001^*$
	BGF18	0.28 (0.25; 0.37)		3.38 (3.41; 4.51)		3.50 (3.35; 4.27)	
Se	Ti	0.09 (0.10; 0.14)	$p = 1.000^*$	0.11 (0.12; 0.24)	$p = 0.107^*$	0.15 (0.16; 0.24)	$p = 0.016^*$
	BGF18	0.10 (0.10; 0.12)		0.11 (0.11; 0.13)		0.12 (0.12; 0.14)	

*Multiple Comparisons - Generalized Linear Model with Bonferroni correction.

Results

The SEM images of titanium (Ti) and F18 Bioactive Glass (BGF18) are shown in Figure 1a–b. Figure 1c refers to the hydroxycarbonate apatite (HCA) layer formed after immersion for 16 h in Simulated Body Fluid. After initial dissolution of the biomaterial, structures like “needles” can be observed on the surface of BGF18 (Figure 1c). A significant increase in surface roughness (R_a) was observed on the titanium covered with BGF18 specimen [3.96 (3.51–4.70)] in comparison with the titanium specimen [0.3 (0.26–0.51)] – (95% confidence interval for mean, $p < 0.001$).

The quantification of live and dead cells on the materials surface, after culture for 2, 4 and 8 h evaluated only the cells stained green (live) since there was interference between BGF18 and the red dye (propidium iodide). This interference was visible even after successive rinsing.

Regarding biofilm formation, the BGF18 specimens had smaller areas, as a percentage, coated with cells after cultivation for 8 h (*C. albicans* $p < 0.001$; *P. aeruginosa* $p < 0.001$; *S. epidermidis* $p = 0.016$). As for the *P. aeruginosa* biofilm, a reduction in areas coated with cells was also detected after incubation for 4 h ($p < 0.001$) (Table 1). For all biofilms, both surfaces seem to be similar in cell adhesion after incubation for 2 h.

The fluorescence microscope (FM) representative biofilm images at 2, 4 and 8 h of culture are shown in Figure 2. The CLSM and SEM representative biofilm images at 24 and 48 h are shown in Figure 3 and 4. At 24 h of cultivation, the biofilm growth seems to be similar on both material surfaces. At 48 h, structures like “towers” could be observed in the *S. epidermidis* and *P. aeruginosa* BGF18 images.

The selected CLSM representative biofilm matrix images at 48 h are shown in Figure 5. A variation in staining patterns was noticed depending on the microorganism. All biofilm matrixes seemed to be thicker on the BGF18 surface [*C. albicans* – 82.94 (11.54); *P. aeruginosa* – 142.94 (16.05); *S. epidermidis* – 113.27(17.50)] than on the titanium surface [*C. albicans* – 64.77 (10.26); *P. aeruginosa* – 57.21 (17.20); *S. epidermidis* – 71.58 (13.73)], $p < 0.001$. The difference between groups is presented in Figure 6.

Discussion

In the present study, titanium coated with F18 Bioactive Glass (BGF18) and plain titanium (Ti) samples were used for evaluation of anti-biofilm activity against *C. albicans*, *P. aeruginosa* and *S. epidermidis* biofilm growth. The null hypothesis was denied since it was observed that there were clear differences in the adhesion, and the biofilm and matrix of polymeric substances, formed after growth for 2, 4 and 8 h.

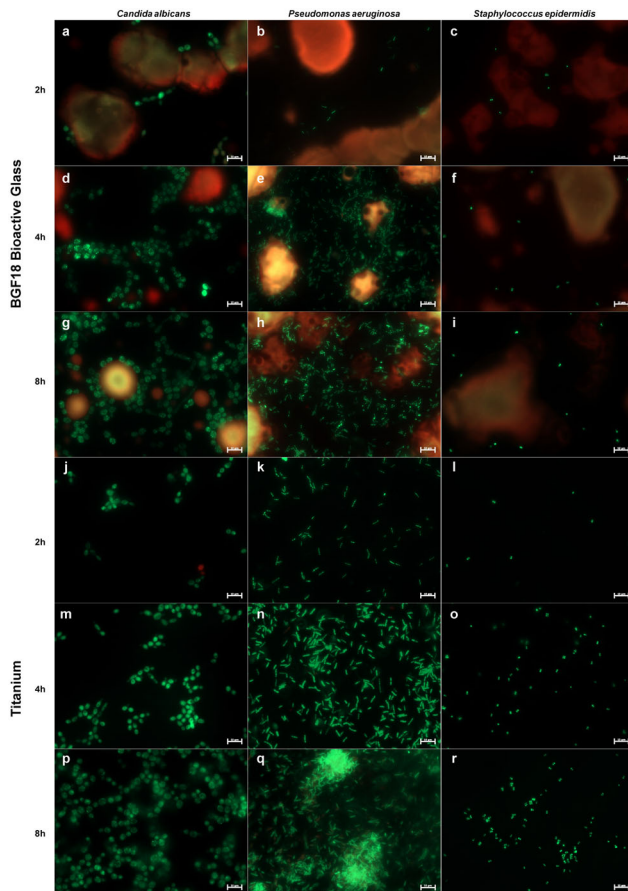


Figure 2. Fluorescence microscope images of *C. albicans* (a, d, g, j, m, p), *P. aeruginosa* (b, e, h, k, n, q) and *S. epidermidis* (c, f, i, l, o, r) viewed after incubation for 2, 4 and 8 h on BGF18 (a–i) and Ti (j–r). The cells were stained with the LIVE/DEAD™ Biofilm Viability Kit dye. Magnification 630 \times . BGF18 specimens had smaller areas, as percentages, coated with cells after cultivation of all the microorganisms tested for 8 h. Scale bars = 10 μ m.

The bioactive glass coating features were chosen based on previous *in vivo* results that showed improved and speedier osseointegration (Soares et al. 2018). Besides the contribution to the osteogenic properties, bioglasses have been investigated for potential anti-biofilm activity in an effort to combat implant-associated infections. Souza et al. (2016a) reported a broad-spectrum antibacterial property of BGF18 against planktonic forms of *S. aureus*, *S. epidermidis*, *P. aeruginosa* and *Escherichia coli* in 24 h of direct contact with the material.

The BGF18 specimens had smaller areas coated with cells of all the microorganisms tested after cultivation for 8 h. Regarding the *P. aeruginosa* biofilm, a reduction in the number of cells was detected at 4 h and 8 h of incubation (Table 1). These results are consistent with those presented by Souza et al. (2016a)

and allowed the authors to infer that biofilm formation was dependent on biomaterials, microorganisms and incubation times. Furthermore, the biofilms formed by *S. epidermidis* covered much smaller areas on the biomaterials than those formed by *C. albicans* and *P. aeruginosa*. This is likely due to the morphological characteristics and the biochemical and metabolic properties of the different microorganisms.

In the first hours of biofilm formation, a decrease in adhesion was observed on the BGF18 specimens. This fact can be explained as a result of the alteration in the microenvironment caused by the dissolution of the biomaterial. Hench (1991) demonstrated that in the first moment that bioactive glass contacts the surrounding body fluids, it causes an increase in pH, resulting in an alkaline microenvironment. The release of sodium, silica, calcium and phosphate from the bioactive glass surface increases salt concentration and osmotic pressure. Moreover, Begum et al. (2016) suggested that the formation of sharp debris as “needles” could damage the walls of microbial cells. The decreased adhesion and growth observed up to 8 h of culture can be justified by these mechanisms as also proposed by Drago et al. (2018). In Figure 1c, it is possible to see those needle-like structures on the surface of BGF18 after immersion for 16 h in Simulated Body Fluid.

For longer experimental periods, growth for 48 h, increased biofilm formation was observed on the BGF18 specimens (Figures 3 and 4). In other words, the biomaterial did not show satisfactory anti-biofilm activity after incubation for 8 h. This can be linked to the dissolution process of the bioactive glass and the total consumption of the active agent, mainly since only a small concentration was used. A coated surface used in this study represents a small amount of BGF18, about 25% of total area, as shown in Figure 1. This would represent a concentration of ~ 1.34 mg ml $^{-1}$ (bioglass/medium). Thus, the ion leaching process from the bioglass particle to the medium cannot lead to a long-time pH alteration, an important feature for the antibacterial activity of bioglasses (Xie et al. 2008; Coraça-Huber et al. 2014).

According to Hao et al. (2018), surface roughness can favor the process of biofilm formation by increasing the contact surface. In this study, a significant increase in surface roughness (Ra) was observed on titanium specimen covered with BGF18 in comparison with titanium ($p < 0.001$). A previous study highlighted that BGF18 could be responsible for a substantial roughness and wettability alteration of the surface (Soares et al. 2018). The increase in surface

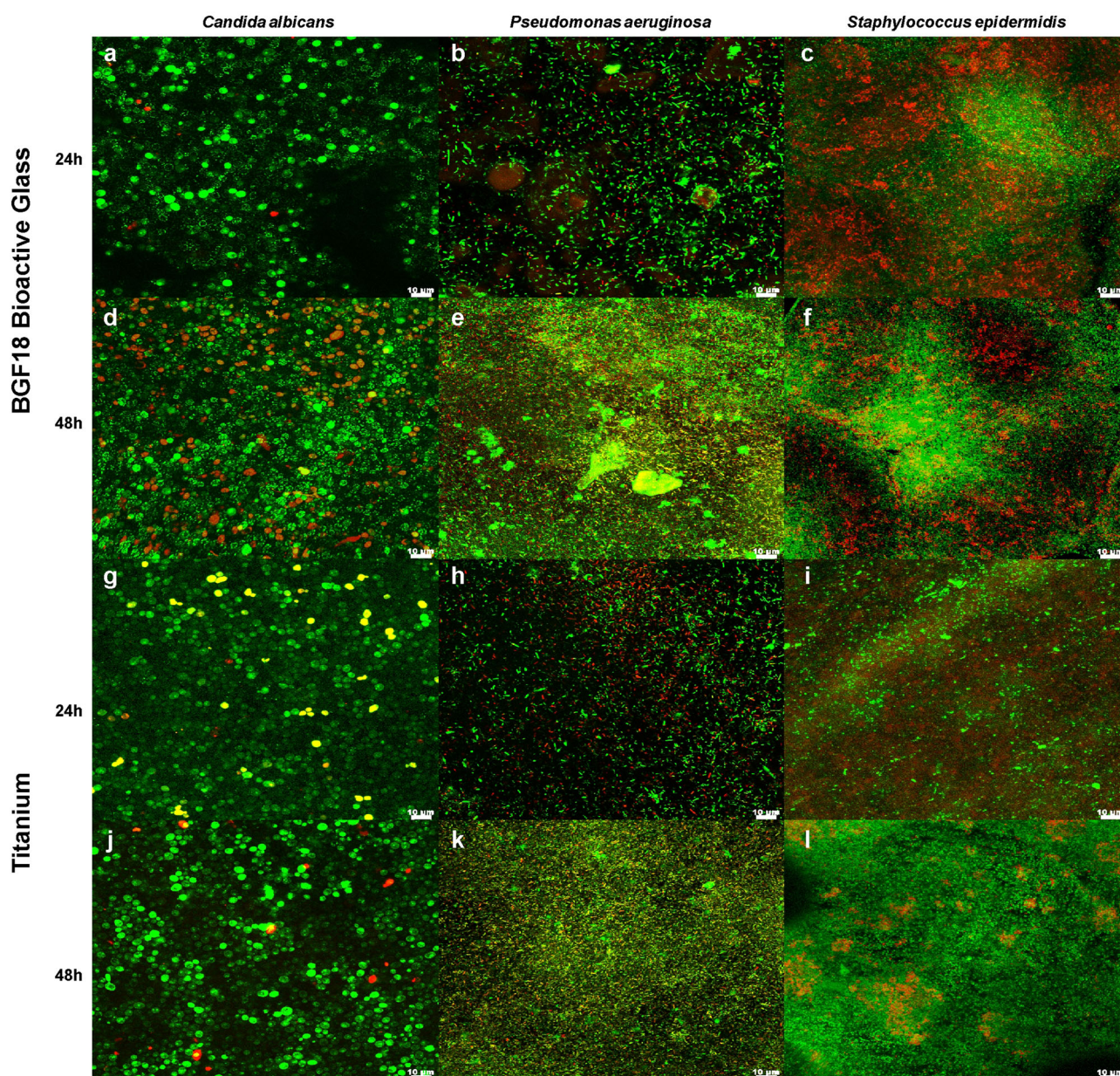


Figure 3. CLSM images of BGF18 (a–f) and Ti (g–l). Biofilms at 24 and 48 h of *C. albicans* (a, d, g, j), *P. aeruginosa* (b, e, h, k) and *S. epidermidis* (c, f, i, l). For FM visualization, the cells were stained with the LIVE/DEAD™ Biofilm Viability Kit dye. Magnification 630×. At cultivation for 24 h, the biofilm growth seemed to be similar on both material surfaces. At 48 h, structures like “towers” could be observed in *S. epidermidis* and *P. aeruginosa* BGF18 images. Scale bars = 10 µm.

roughness could have favored biofilm formation after 8 h suggesting that cell adhesion had started on the free surface and after the formation of the mineralized hydroxyapatite layer, reached the remaining areas. The interaction between bioglass particles and bacterial cell membranes is crucial for a biocidal effect (Cabal et al. 2011). As the BGF18 coating covered 25% of total area of the specimen, the contact between the biomaterial and cells membranes was compromised.

Additionally, when any bioactive glass is exposed to any aqueous solution, it undergoes reactions that

lead to the formation of a carbonated hydroxyapatite (HCA) layer on its surface (Souza et al. 2016b, 2017; Baino et al. 2018). The development of this HCA layer is a desired feature in all inorganic materials in bone replacement, orthopedic implants and repair of bone tissue. HCA layer formation is a condition seen as necessary for the development of a chemical bond between bone and the biomaterial (Hench 2013). A study conducted by Souza et al. (2017) analyzed the reaction of BGF18 when exposed to a substance like human blood plasma (Simulated Body Fluid solution). Infrared spectroscopy images showed HCA layer

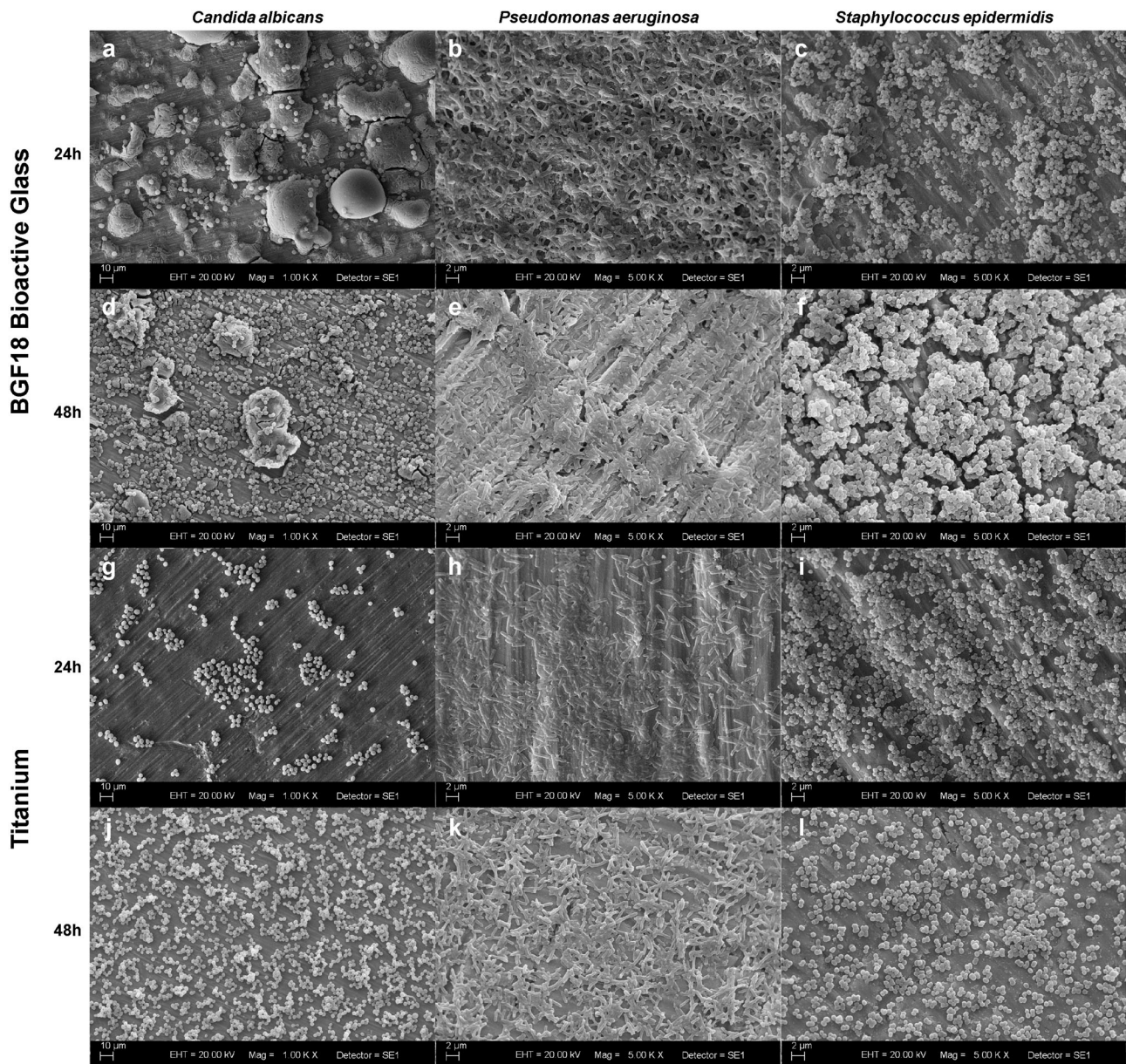


Figure 4. SEM images of BGF18 (a–f) and Ti (g–l). Biofilms at 24 and 48 h of *C. albicans* (a, d, g, j - magnification 1,000×, scale bar = 10 μm), *P. aeruginosa* (b, e, h, k - magnification 5,000×, scale bar = 2 μm) and *S. epidermidis* (c, f, i, l - magnification 5,000×, scale bars = 2 μm).

formation after 4 and 12 h, which was favorable for bone regeneration. HCA-coating has been frequently related to stabilizing, protecting and delivering molecules (Fulgione et al. 2019; Türe 2019; Yang et al. 2019), mainly due to its biocompatibility and lack of antimicrobial activity. BGF18 progressed to a mineralized hydroxyapatite layer after only 4 to 12 h, when immersed in a Simulated Body Fluid solution, as shown by Gabbai-Armelin et al. (2017) and Souza et al. (2017). Thus, in this study, the absence of an antimicrobial effect of HCA might have favor colonization at 24 and 48 h by surface topographical irregularities.

Anti-biofilm activity on surfaces coated with bioactive glass has been reported in the literature; however, these studies are widely heterogeneous regarding the bacterial species tested, methods of analysis, as well as the composition, size and concentration of the bioactive glass used (Coraça-Huber et al. 2014; Drago et al. 2018). In this study, after growth for 48 h, a large amount of biofilm matrix substances was observed on the BGF18 specimens. All biofilm matrixes seemed to be thicker on the BGF18 surface than on the titanium surfaces ($p < 0.001$). This feature may be due to the morphological and structural responses of the microorganisms, modifying the

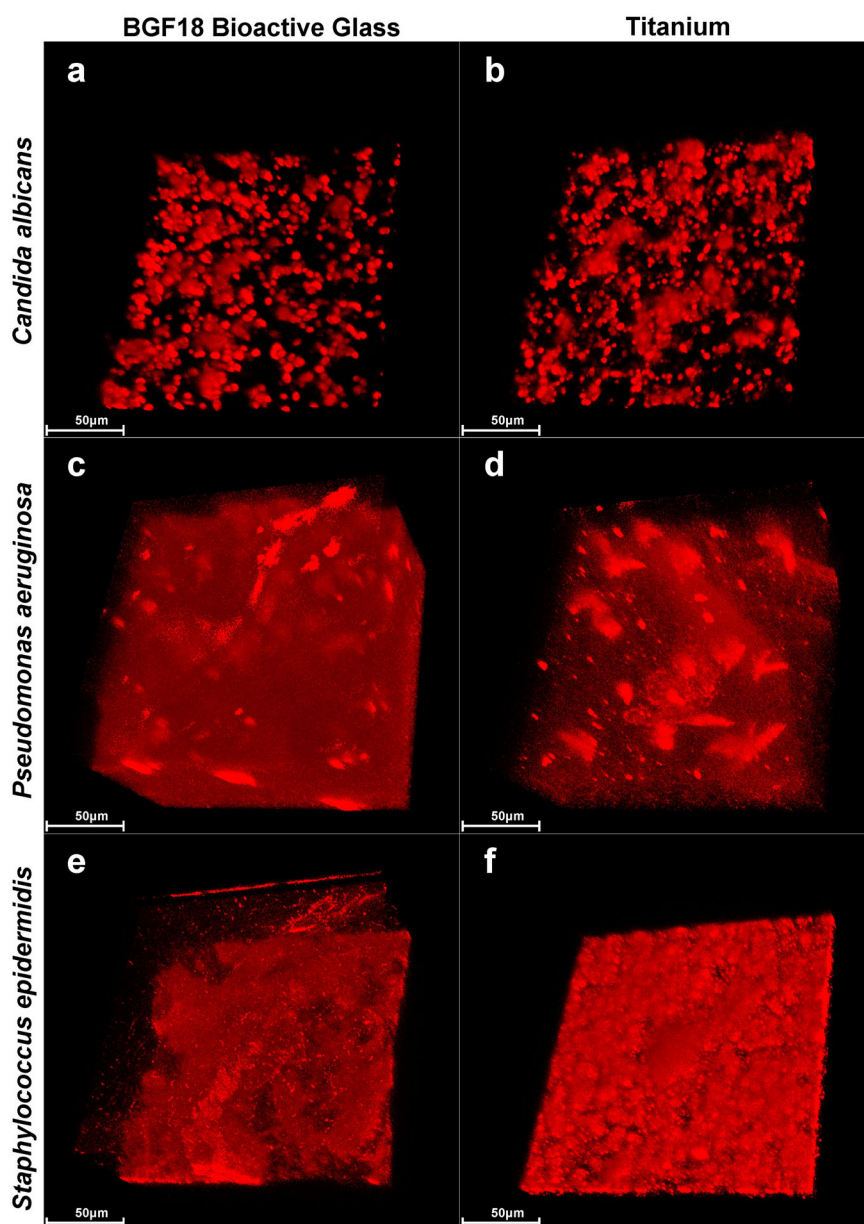


Figure 5. CLSM 3-D images of the biofilm matrix at 48 h of *C. albicans* (a, b), *P. aeruginosa* (c, d) and *S. epidermidis* (e, f), grown on BGF18 (a, c, e) and Ti surfaces (b, d, f). All biofilm matrixes seemed to be thicker on BGF18 surfaces. Scale bar = 50 μm .

expression pattern of numerous genes and proteins in presence of BGF18 (Ran et al. 2013). Bacteria can coordinate the expression of their virulence determinants according to adaptive response in replaying environmental alterations, such as concentrations of ions and pH (Thomas and Wigneshweraraj 2014). Chang et al. (2005) observed an alteration of virulence factors, as a defense mechanisms in *P. aeruginosa*, in responses to oxidative stress. Calcium addition resulted in thicker *P. aeruginosa* biofilms with increased alginate and extracellular proteases secretion (Sarkisova et al. 2005). Drago et al. (2015) demonstrated that morphological changes are induced in *S. epidermidis*, *Acinetobacter baumannii* and *Klebsiella*

pneumoniae strains after incubation with bioactive glass. By inspecting Biofilm matrix thickness values, the calcium and phosphate ions released by BGF18 to the medium, and their post consumption for hydroxyapatite layer formation, as demonstrated by Souza et al. (2016a), have a significant impact on the development of a mature biofilm structure promoting both morphological and phenotypic changes in the microorganisms.

Even though a decrease in microbial growth was only seen up to 8 h of cultivation, it is believed that this result is important and promising, since even using such a small concentration as 1.34 mg ml^{-1} , anti-biofilm action could be observed. Coraça-Huber

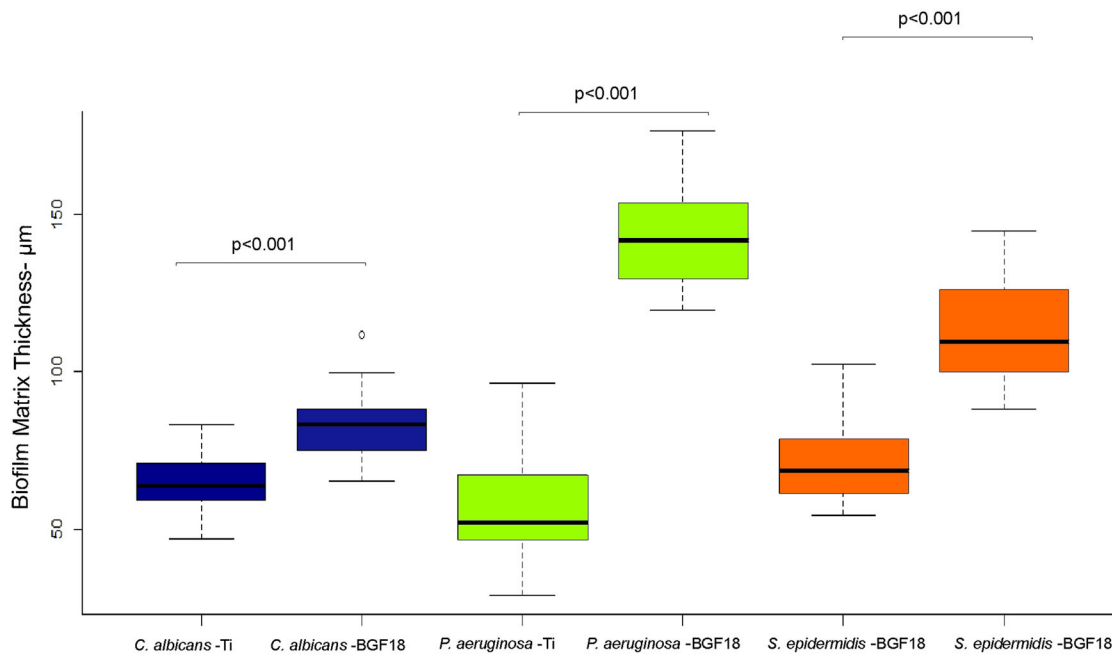


Figure 6. Boxplot chart representing biofilm matrix measurements of *C. albicans*, *P. aeruginosa* and *S. epidermidis* biofilms, grown on titanium (Ti) and titanium coated with F18 Bioactive Glass (BGF18). Test t-Student – $p < 0.001$.

et al. (2014) reported that S53P4 bioactive glass could suppress biofilm formation on titanium discs *in vitro* by using 500 mg l^{-1} of bioactive glass. This amount is significantly higher than that used in this study. So, BGF18 on the implant surface initially reduced microorganism adhesion and has the ability to induce the formation of bone and blood vessel tissue (Souza et al. 2016a; Soares et al. 2018). These factors, combined with the patient's immune response and antibiotic therapy, might reduce the biofilm formation process. Furthermore, it is worth noting that the initial inoculum used in *in vitro* studies is immensely larger than the number of microorganisms available in circulation or at the time of installation of a prosthesis in a patient. The reduction in adhesion starting at 10^6 CFU ml^{-1} is significant since some studies have shown that the contamination of prosthesis was below this value (Liu et al. 2017).

New studies involving the alteration in the morphological and ultrastructural characteristics beyond the pattern of gene and protein expression are important to determine the mechanisms of action of BGF18 on the growth of microorganisms. It is worth noting the importance of evaluating adhesion, quorum sensing and virulence factor-related gene expression on biofilm growth on BGF18 and Ti surfaces. Moreover, the development of new coating approaches or deposition of bioactive glass on surfaces is urgent, in order to cope with the rapid dissolution and bioactivity of the material. The use of

bioactive glass as a support for incorporation and vehicles for the controlled release of therapeutic ions and molecules, such as osteogenesis and angiogenesis stimulants, antimicrobials, anti-inflammatories and anticancer drugs, has been tested in order to improve their biological activities (Garg et al. 2017; Baino et al. 2018). These approaches emerge as a new horizon for dealing with infections in implants caused by biofilms and emphasize that research involving bioactive glasses requires interdisciplinary collaboration.

As a limitation of the study, measurement of red-stained cells was not satisfactory because the dye also impregnated on the BGF18 particles. This problem renders the separation of dead cells from the background in fluorescence microscope images impossible. Further studies on the interaction of the dye with the BGF18 particles are necessary to improve the understanding of the said phenomena.

Conclusion

Within the limitations of this study, the new F18 Bioactive Glass presented less biofilm formation than titanium up to 8 h of incubation, even when using low concentrations, such as 1.34 mg ml^{-1} . However, after incubation for 48 h, there was extensive microbial growth and matrix production, possibly due to the glass consumption and the subsequent formation of the HCA layer. The results obtained indicate a good ability of F18 Bioactive Glass to control and

prevent infections *in situ* even when presented in small concentrations.

Disclosure statement


No potential conflict of interest was reported by the author(s).

Funding

This work was supported by FAPESP (São Paulo Research Foundation) under grants number [2018/17073-4 and 2013/07793-6] and CAPES (Coordination for the Improvement of Higher Education Personnel – Brazil) [Finance Code 001].

ORCID

Daniella Maia Marques  <http://orcid.org/0000-0002-0247-7801>

Viviane de Cássia Oliveira  <http://orcid.org/0000-0002-0734-0652>

Marina Trevelin Souza  <http://orcid.org/0000-0002-0291-6034>

Edgar Dutra Zanotto  <http://orcid.org/0000-0003-4931-4505>

João Paulo Mardegan Issa  <http://orcid.org/0000-0002-1056-0795>

Evandro Watanabe  <http://orcid.org/0000-0001-5674-2589>

Data availability statement

The raw/processed data required to reproduce these findings cannot be shared at this time as the data are also part of an ongoing study.

References

- Baino F, Hamzehlou S, Kargozar S. 2018. Bioactive glasses: where are we and where are we going? *JFB*. 9:25. doi: [10.3390/jfb9010025](https://doi.org/10.3390/jfb9010025)
- Begum S, Johnson WE, Worthington T, Martin RA. 2016. The influence of pH and fluid dynamics on the antibacterial efficacy of 45S5 Bioglass. *Biomed Mater*. 11:015006. doi: [10.1088/1748-6041/11/1/015006](https://doi.org/10.1088/1748-6041/11/1/015006)
- Cabal B, Malpartida F, Torrecillas R, Hoppe A, Boccaccini AR, Moya JS. 2011. The development of bioactive glass-ceramic substrates with biocide activity. *Adv Eng Mater*. 13:462–466. doi: [10.1002/adem.201180026](https://doi.org/10.1002/adem.201180026)
- Chang W, Small DA, Toghrol F, Bentley WE. 2005. Microarray analysis of *Pseudomonas aeruginosa* reveals induction of pyocin genes in response to hydrogen peroxide. *BMC Genomics*. 6:1–14. doi: [10.1186/1471-2164-6-115](https://doi.org/10.1186/1471-2164-6-115)
- Cochis A, Azzimonti B, Della Valle C, De Giglio E, Bloise N, Visai L, Cometa S, Rimondini L, Chiesa R. 2016. The effect of silver or gallium doped titanium against the multidrug resistant *Acinetobacter baumannii*. *Biomaterials*. 80:80–95. doi: [10.1016/j.biomaterials.2015.11.042](https://doi.org/10.1016/j.biomaterials.2015.11.042)
- Coraça-Huber DC, Fille M, Hausdorfer J, Putzer D, Nogler M. 2014. Efficacy of antibacterial bioactive glass S53P4 against *S. aureus* biofilms grown on titanium discs in vitro. *J Orthop Res*. 32:175–177. doi: [10.1002/jor.22463](https://doi.org/10.1002/jor.22463)
- Drago L, De Vecchi E, Bortolin M, Toscano M, Mattina R, Romanò CL. 2015. Antimicrobial activity and resistance selection of different bioglass S53P4 formulations against multidrug resistant strains. *Future Microbiol*. 10:1293–1299. doi: [10.2217/FMB.15.57](https://doi.org/10.2217/FMB.15.57)
- Drago L, Toscano M, Bottagisio M. 2018. Recent evidence on bioactive glass antimicrobial and antibiofilm activity: a mini-review. *Materials (Basel)*. 11:326. doi: [10.3390/ma11020326](https://doi.org/10.3390/ma11020326)
- Fulgione A, Ianniello F, Papaiani M, Contaldi F, Sgamma T, Giannini C, Pastore S, Velotta R, Della Ventura B, Roveri N, et al. 2019. Biomimetic hydroxyapatite nanocrystals are an active carrier for *Salmonella* bacteriophages. *IJN*. 14:2219–2232. doi: [10.2147/IJN.S190188](https://doi.org/10.2147/IJN.S190188)
- Gabbai-Armelin PR, Souza MT, Kido HW, Tim CR, Bossini PS, Fernandes KR, Magri AM, Parizotto NA, Fernandes KP, Mesquita-Ferrari RA, et al. 2017. Characterization and biocompatibility of a fibrous glassy scaffold. *J Tissue Eng Regen Med*. 11:1141–1151. doi: [10.1002/term.2017](https://doi.org/10.1002/term.2017)
- Gao AR, Hang X, Huang L, Zhao X, Zhang L, Wang L, Tang B, Ma S, Chu PK. 2014. The effects of titania nanotubes with embedded silver oxide nanoparticles on bacteria and osteoblasts. *Biomaterials*. 35:4223–4235. doi: [10.1016/j.biomaterials.2014.01.058](https://doi.org/10.1016/j.biomaterials.2014.01.058)
- Garg S, Thakur S, Gupta A, Kaur G, Pandey OP. 2017. Antibacterial and anticancerous drug loading kinetics for (10-x)CuO-xZnO-20CaO-60SiO₂-10P₂O₅ (2 ≤ x ≤ 8) mesoporous bioactive glasses. *J Mater Sci Mater Med*. 28:11. doi: [10.1007/s10856-016-5827-x](https://doi.org/10.1007/s10856-016-5827-x)
- Hao Y, Huang XY, Zhou XD, Li MY, Ren B, Peng X, Cheng L. 2018. Influence of dental prosthesis and restorative materials interface on oral biofilms. *IJMS*. 19:3157. doi: [10.3390/ijms19103157](https://doi.org/10.3390/ijms19103157)
- Hench LL, Splinter RJ, Allen WC, Greenlee TK. 1971. Bonding mechanisms at the interface of ceramic prosthetic materials. *J Biomed Mater Res*. 5:117–141. doi: [10.1002/jbm.820050611](https://doi.org/10.1002/jbm.820050611)
- Hench LL. 1991. Bioceramics: from concept to clinic. *J Am Ceramic Society*. 74:1487–1510. doi: [10.1111/j.1151-2916.1991.tb07132.x](https://doi.org/10.1111/j.1151-2916.1991.tb07132.x)
- Hench LL. 2013. An Introduction to bioceramics. 2nd ed. London: Imperial College Press.
- Kargozar S, Hamzehlou S, Baino F. 2017. Potential of bioactive glasses for cardiac and pulmonary tissue engineering. *Materials (Basel)*. 10:1429. doi: [10.3390/ma10121429](https://doi.org/10.3390/ma10121429)
- Kragh KN, Hutchison JB, Melaugh G, Rodesney C, Roberts AEL, Irie Y, Jensen PO, Diggle SP, Allen RJ, Gordon V, et al. 2016. Role of multicellular aggregates in biofilm formation. *MBio*. 7:e00237. doi: [10.1128/mBio.00237-16](https://doi.org/10.1128/mBio.00237-16)
- Kuehl R, Brunetto PS, Woischinig AK, Varisco M, Rajacic Z, Vosbeck J, Terracciano L, Fromm KM, Khanna N. 2016. Preventing implant-associated infections by silver coating. *Antimicrob Agents Chemother*. 60:2467–2475. doi: [10.1128/AAC.02934-15](https://doi.org/10.1128/AAC.02934-15)

- Liu H, Zhang Y, Li L, Zou C. 2017. The application of sonication in diagnosis of periprosthetic joint infection. *Eur J Clin Microbiol Infect Dis.* 36:1–9. doi: [10.1007/s10096-016-2778-6](https://doi.org/10.1007/s10096-016-2778-6)
- Macia MD, Rojo-Molinero E, Oliver A. 2014. Antimicrobial susceptibility testing in biofilm-growing bacteria. *Clin Microbiol Infect.* 20:981–990. doi: [10.1111/1469-0691](https://doi.org/10.1111/1469-0691)
- Miguez-Pacheco V, Greenspan D, Hench LL, Boccaccini AR. 2015. Bioactive glasses in soft tissue repair. *Am Ceram Soc Bull.* 13:1–31. doi: [10.1016/j.actbio.2014.11.004](https://doi.org/10.1016/j.actbio.2014.11.004)
- Ran S, He Z, Liang J. 2013. Survival of *Enterococcus faecalis* during alkaline stress: changes in morphology, ultrastructure, physicochemical properties of the cell wall and specific gene transcripts. *Arch Oral Biol.* 58:1667–1676. doi: [10.1016/j.archoralbio.2013.08.013](https://doi.org/10.1016/j.archoralbio.2013.08.013)
- Sarkisova S, Patrauchan MA, Berglund D, Nivens DE, Franklin MJ. 2005. Calcium-induced virulence factors associated with the extracellular matrix of mucoid *Pseudomonas aeruginosa* biofilms. *JB.* 187:4327–4337. doi: [10.1128/JB.187.13.4327-4337.2005](https://doi.org/10.1128/JB.187.13.4327-4337.2005)
- Soares PBF, Moura CCG, Chinaglia CR, Zanotto ED, Zanetta-Barbosa D, Stavropoulos A. 2018. Effect of titanium surface functionalization with bioactive glass on osseointegration: an experimental study in dogs. *Clin Oral Implants Res.* doi: [10.1111/clr.13375](https://doi.org/10.1111/clr.13375)
- Souza MT, Campanini LA, Chinaglia CR, Peitl O, Zanotto ED, Souza C. 2016a. Broad-spectrum bactericidal activity of a new bioactive grafting material (F18) against clinically important bacterial strains. *Int J Antimicrob Agents.* 50:730–733. doi: [10.1016/j.ijantimicag.2017.08.015](https://doi.org/10.1016/j.ijantimicag.2017.08.015)
- Souza MT, Peitl O, Zanotto ED, Boccaccini AR. 2016b. Novel double-layered conduit containing highly bioactive glass fibers for potential nerve guide application. *Int J Appl Glass Sci.* 7:183–194. doi: [10.1111/ijag.12208](https://doi.org/10.1111/ijag.12208)
- Souza MT, Rennó ACM, Peitl O, Zanotto ED. 2017. New highly bioactive crystallization-resistant glass for tissue engineering applications. *Transl Mater Res.* 4:014002. doi: [10.1088/2053-1613/aa53b5](https://doi.org/10.1088/2053-1613/aa53b5)
- Thomas MS, Wigneshweraraj S. 2014. Regulation of virulence gene expression. *Virulence.* 5:832–834. doi: [10.1080/21505594.2014.995573](https://doi.org/10.1080/21505594.2014.995573)
- Türe H. 2019. Characterization of hydroxyapatite-containing alginate–gelatin composite films as a potential wound dressing. *Int J Biol Macromol.* 123:878–888. doi: [10.1016/j.ijbiomac.2018.11.143](https://doi.org/10.1016/j.ijbiomac.2018.11.143)
- West S, Horn H, Hijnen WAM, Castillo C, Wagner M. 2014. Confocal laser scanning microscopy as a tool to validate the efficiency of membrane cleaning procedures to remove biofilms. *Sep Purif Technol.* 122:402–411. doi: [10.1016/j.seppur.2013.11.032](https://doi.org/10.1016/j.seppur.2013.11.032)
- Xie ZP, Zhang CQ, Yi CQ, Qiu JJ, Wang JQ, Zhou J. 2008. *In vivo* study effect of particulate bioglass (R) in the prevention of infection in open fracture fixation. *J Biomed Mater Res.* 90B:195–201. doi: [10.1002/jbm.b.31273](https://doi.org/10.1002/jbm.b.31273)
- Yang Y, Xia L, Haapasalo M, Wei W, Zhang D, Ma J, Shen Y. 2019. A novel hydroxyapatite-binding antimicrobial peptide against oral biofilms. *Clin Oral Invest.* 23:2705–2712. doi: [10.1007/s00784-018-2701-x](https://doi.org/10.1007/s00784-018-2701-x)